Supporting Information for

Micelles Embedded in Multiphasic Protein Hydrogel Enable Efficient and Air-Tolerant Triplet Fusion Upconversion with Heavy-Atom and Spin-Orbit Charge-Transfer Sensitizers

Alexander M. Oddo,[a] Tomoyasu Mani,[a]* Challa V. Kumar[a,b,c]*

[a]Department of Chemistry, University of Connecticut, 55 North Eagleville Road, Storrs, CT 06269, USA

[b]Department of Molecular and Cell Biology, University of Connecticut, 91 North Eagleville Road, Storrs, CT 06269, USA

[c]The Institute of Materials Science, University of Connecticut, 97 North Eagleville Road, Storrs, CT 06269, USA

**To whom correspondance should be addressed:*

Email: tomoyasu.mani@uconn.edu ; challa.kumar@uconn.edu

Phone: (860) 486-6721 ; (860) 486-3213

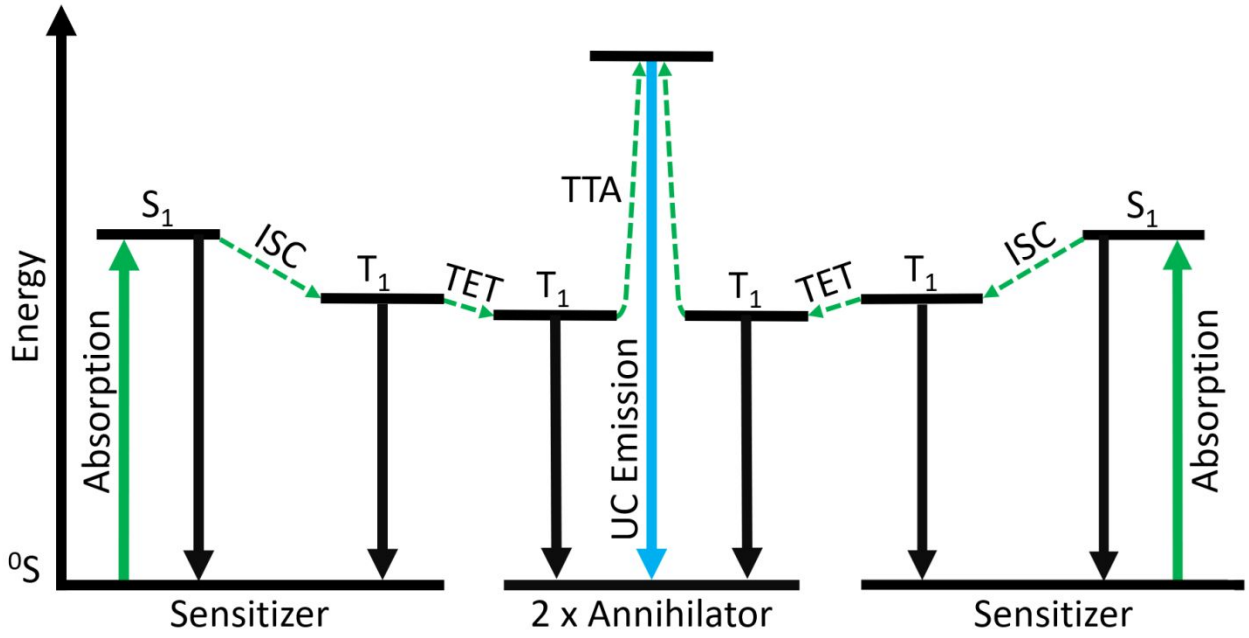

Figure S1. Simplified Jablonski diagram of the TTA-UC mechanism. The depicted energy levels are ground states (S_0), singlet excited states (S_1), and triplet excited states (T_1). Processes that lead to successful TTA-UC emission are colored green and decay pathways are colored black. Undesired processes, such as sensitizer fluorescence and nonradiative decay of annihilator singlets, are typically minimized by selecting a sensitizer with high intersystem crossing (ISC) efficiency and an annihilator with high fluorescence yield, respectively. In TTA-UC, the absorption of low-energy light generates a sensitizer singlet, which is then converted into a sensitizer triplet through ISC. Next, triplet energy transfer (TET) between the sensitizer triplet and a ground state annihilator via the Dexter mechanism produces a ground state sensitizer and an annihilator triplet. Finally, the triplet-triplet annihilation (TTA) of two acceptor triplets yields a high-energy annihilator singlet from which delayed TTA-UC emission may be observed.

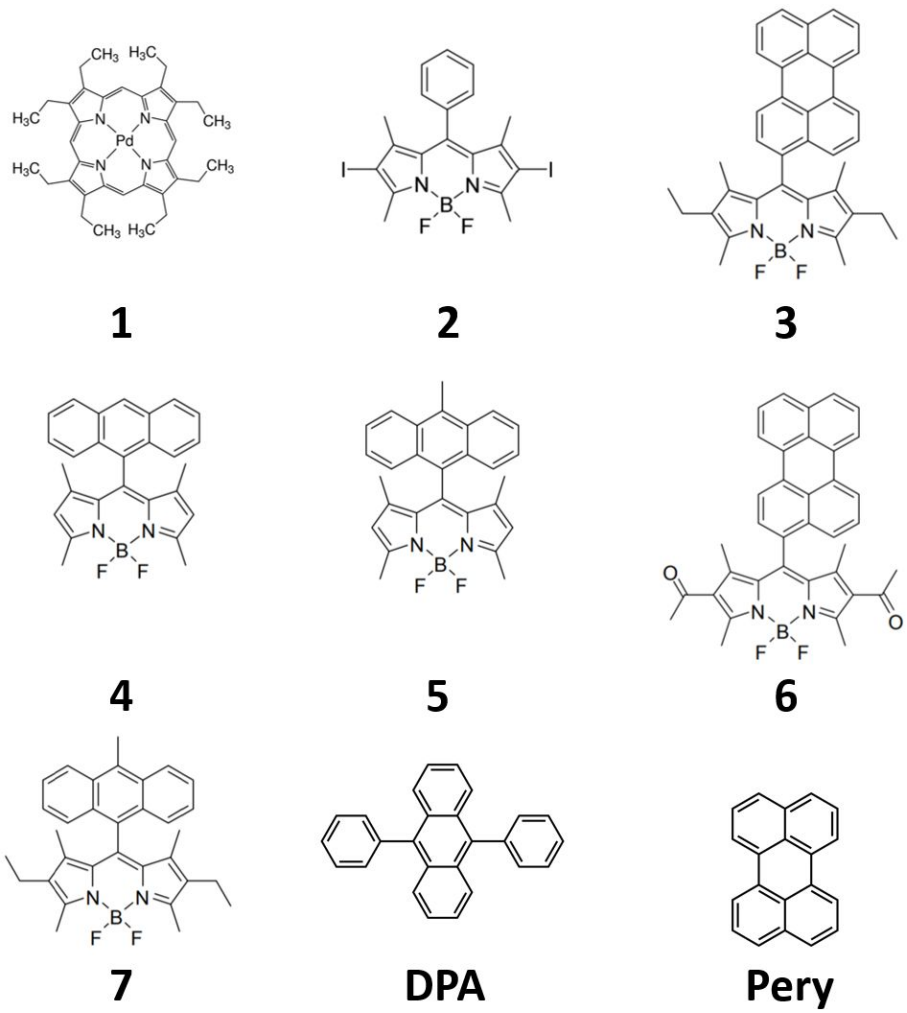

Figure S2. The upconverters used throughout this study. **1-6** were successful TTA-UC sensitizers; **7** was an unsuccessful TTA-UC sensitizer; DPA was the annihilator for **1**; Pery was the annihilator for **2**-**7**.

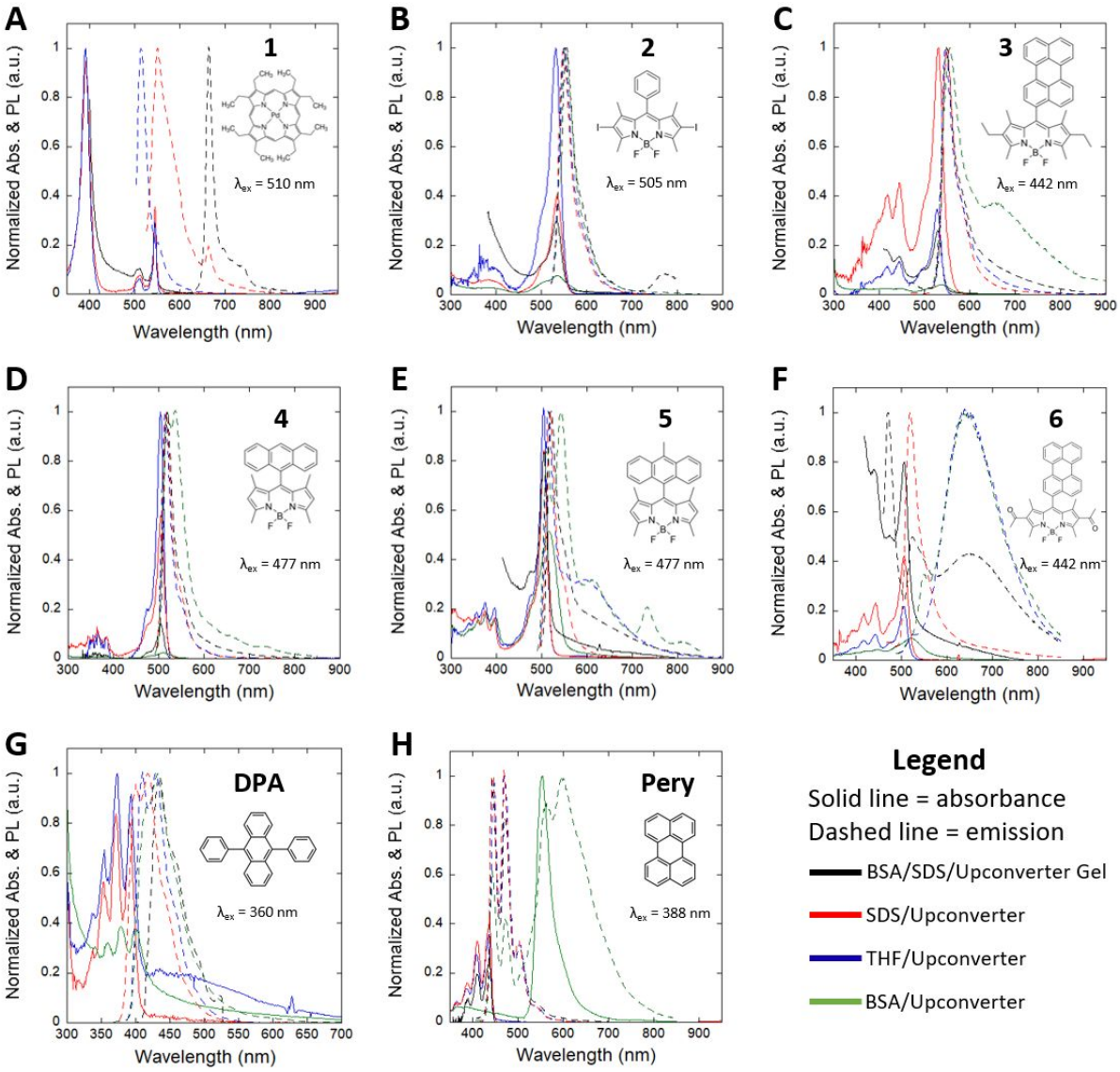

Figure S3. The normalized absorbance and emission spectra of each upconverter (A-H) in various environments; BSA/SDS gel, SDS micelle, THF solution, and BSA complex. The concentrations of a particular upconverter were the same across each of the different environments. The photoexcitation of individual upconverters resulted in Stokes shifted emission in each case. The above data were measured under aerobic conditions at room temperature.

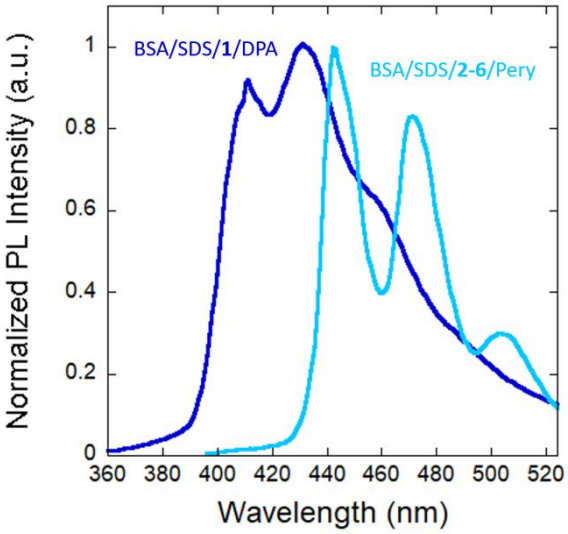

Figure S4. Representative normalized TTA-UC emission spectra of BSA/SDS/**1**/DPA and BSA/SDS/**2**-**6**/Pery hydrogels upon photoexcitation at 532 nm with a Xe arc lamp. The above spectra were measured under aerobic conditions at room temperature.

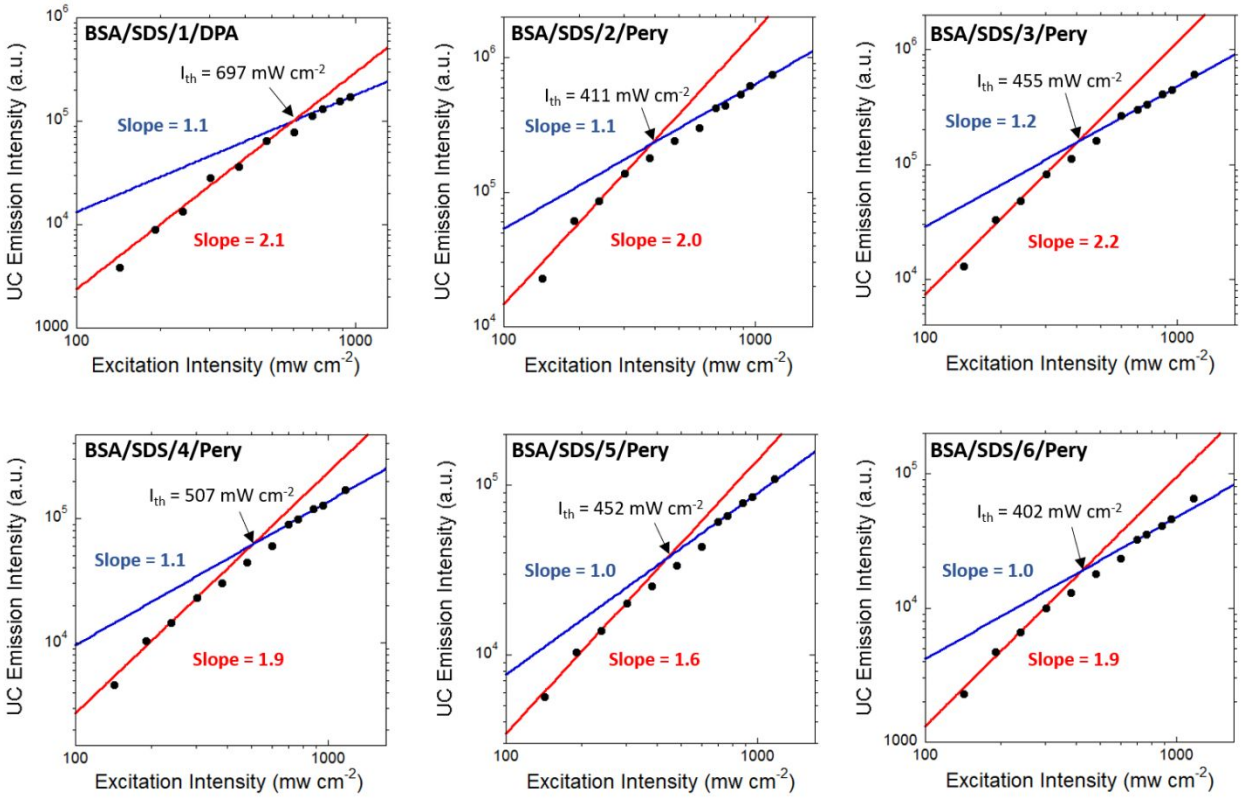

Figure S5. Double logarithmic plots showing the nonlinear dependence of TTA-UC on the 532 nm laser excitation intensity. Each plot corresponds to a particular sensitizer/annihilator pair in the BSA/SDS hydrogel. The solid lines are linear fits performed on the low power (red) and high power (blue) excitation regimes. The above data were measured under aerobic conditions at room temperature.

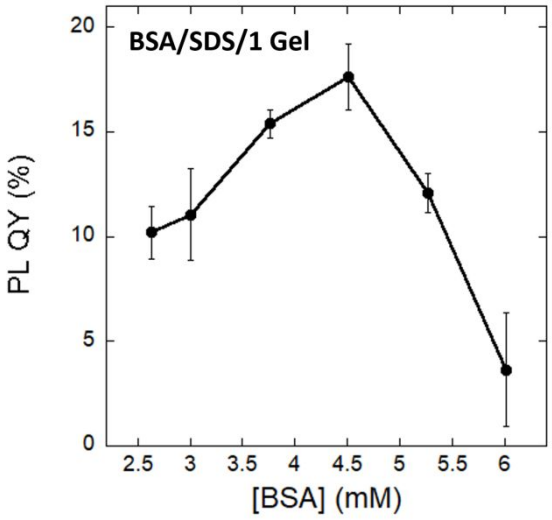

Figure S6. The relationship between the photoluminescence quantum yield (PL QY, Φ_{PL}) of **1** and the concentration of BSA in the BSA/SDS hydrogel. The precipitation of BSA was observed at 5.3 mM. The above data were measured under aerobic conditions at room temperature.

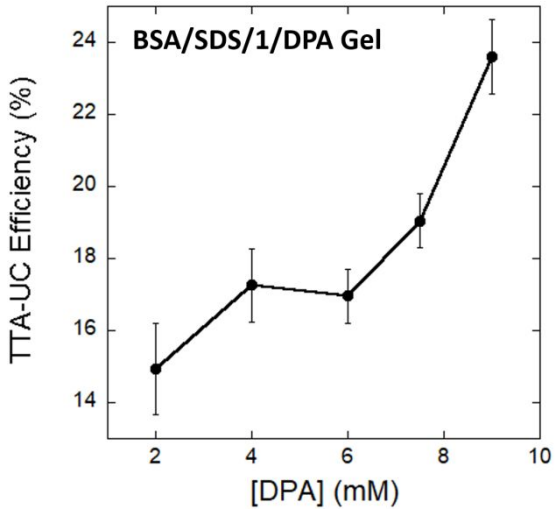

Figure S7. The relationship between the TTA-UC efficiency (Φ_{UC}) and the concentration of DPA in the BSA/SDS/**1**/DPA hydrogel, containing [BSA] = 4.5 mM and [**1**] = 21.2 μM. The precipitation of DPA was observed in the hydrogel at [DPA] = 9 mM, but no aggregation or precipitation was observed at [DPA] = 7.5 mM. The above data were measured under aerobic conditions at room temperature.

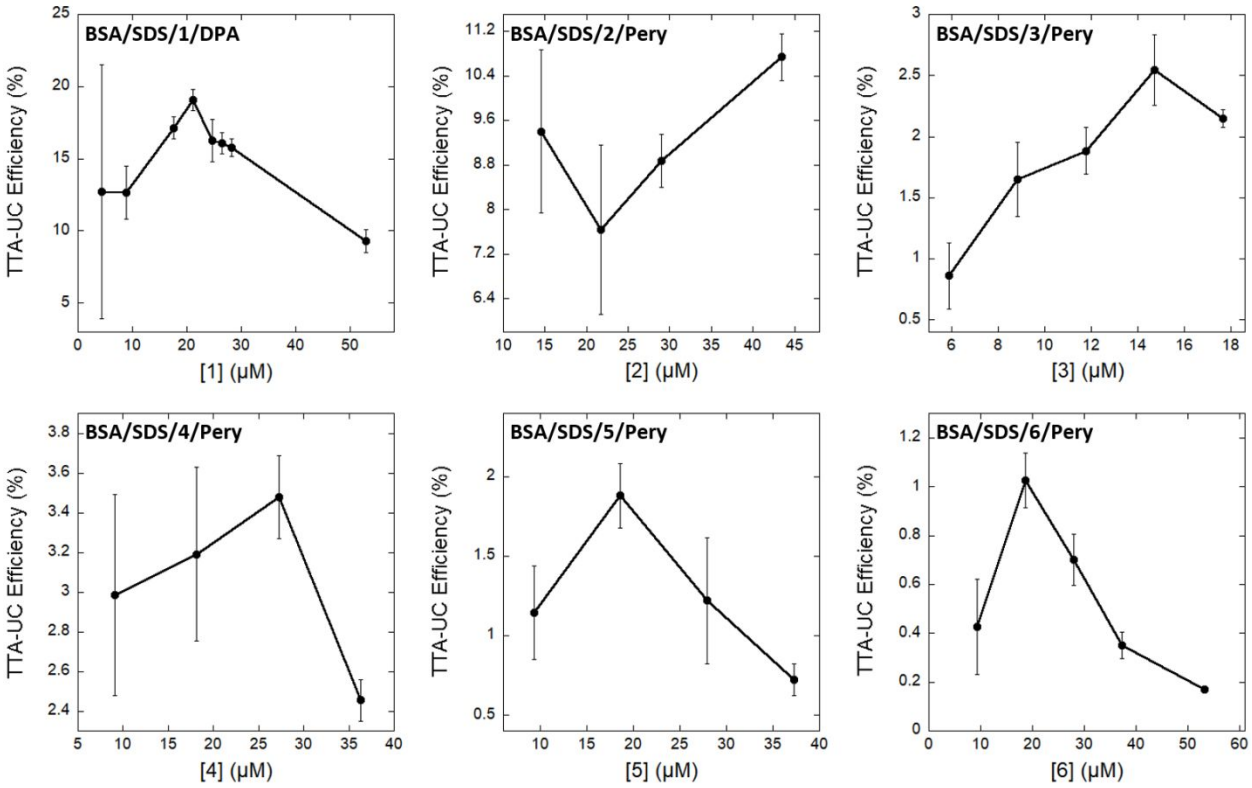

Figure S8. The relationship between the Φ_{UC} and the concentration of sensitizer (**1**-**6**). For the BSA/SDS/**1**/DPA hydrogel, [BSA] = 4.5 mM and [DPA] = 7.5 mM. For the BSA/SDS/**2**-**6**/Pery hydrogels, [BSA] = 4.5 mM and [Pery] = 3.0 mM. The absorbance of each sensitizer concentration was below 1 at λ_{ex} = 532 nm. The 532 nm laser excitation power at which these Φ_{UC} were determined was 7.4 W cm^{-2}. Since photobleaching of the sensitizers was observed over the timescale a full spectral measurement, the TTA-UC emission and sensitizer photoluminescence recorded at a single wavelength under high-intensity laser excitation was measured, which was quick enough to avoid photobleaching. Then, TTA-UC emission and sensitizer photoluminescence spectra were recorded under low-intensity xenon lamp excitation. Finally, these spectra were scaled accordingly to the high-intensity excitation intensity emission results and used in the calculation of Φ_{UC}.

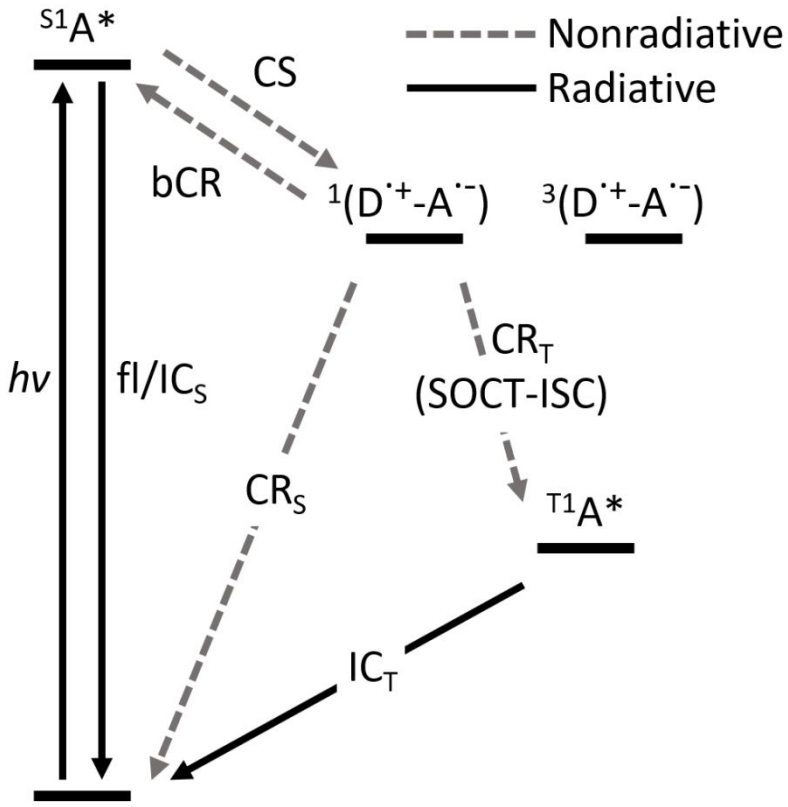

Figure S9. Simplified Jablonski diagram showing spin-orbit charge-transfer intersystem crossing (SOCT-ISC). Fl/IC_S represents fluorescence and internal conversion from the singlet excited state $^{S1}A^*$ to the ground state D–A; CS is charge separation from $^{S1}A^*$ to the charge-separated singlet state $^1(D^{\bullet+}–A^{\bullet-})$; bCR is backwards charge recombination from $^1(D^{\bullet+}–A^{\bullet-})$ to $^{S1}A^*$; CR_S is charge recombination from $^1(D^{\bullet+}–A^{\bullet-})$ to the ground state D–A; CR_T is charge recombination, or SOCT-ISC, from $^1(D^{\bullet+}–A^{\bullet-})$ to the triplet excited state $^{T1}A^*$; IC_T is internal conversion from $^{T1}A^*$ to the ground state D–A; and the charge-separated triplet state is $^3(D^{\bullet+}–A^{\bullet-})$.

A

Sensitizer (solvent)	Φ_{PL} (%)	Φ_T (%)
1 (toluene)	50	~100
2 (toluene)	3	95
3 (MeCN)	1	33
4 (MeCN)	1	93
5 (MeCN)	5	90
6 (MeCN)	1	0.5
7 (MeCN)	10	61

B

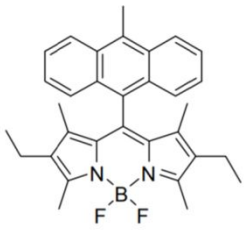

7

BSA/SDS/**7**/Pery: No TTA-UC

BSA/SDS/**7** Φ_{PL} : 60 ± 1.0%

Figure S10. (**A**) Collection of Φ_{PL} and triplet quantum yield (Φ_T) values for **1**-**7** in the specified organic solvents. (**B**) The structure of **7**, which did not produce any TTA-UC emission in the presence of Pery in the BSA/SDS hydrogel. These quantum yields were reported by references [1-3].

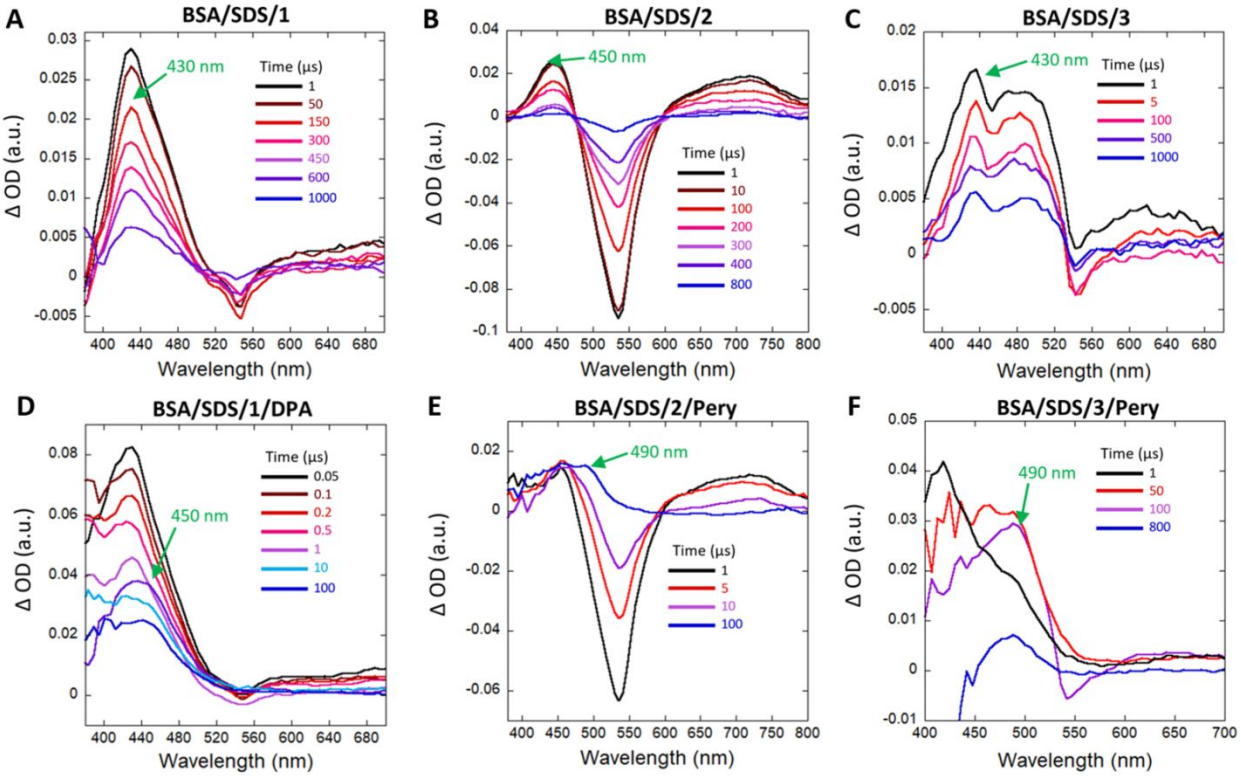

Figure S11. The transient absorption spectra of: (**A**) BSA/SDS/**1**, (**B**) BSA/SDS/**2**, (**C**) BSA/SDS/**3**, (**D**) BSA/SDS/**1**/DPA, (**E**) BSA/SDS/**2**/Pery, and (**F**) BSA/SDS/**3**/Pery recorded taken at certain timescales following the 532 nm laser excitation source. The optimized reagent concentrations were used in each sample: [BSA] = 4.5 mM, [**1**] = 21.2 μM, [**2**] = 43.5 μM, [**3**] = 14.7 μM, [DPA] = 7.5 mM, and [Pery] = 3 mM. The T_1 bands of sensitizers in the BSA/SDS/**1-3** hydrogels and the and T_1 bands of annihilators in the BSA/SDS/**1**/DPA, BSA/SDS/**2**/Pery, and BSA/SDS/**3**/Pery hydrogels are pointed out with a green arrow. The above date were measured under aerobic conditions at room temperature.

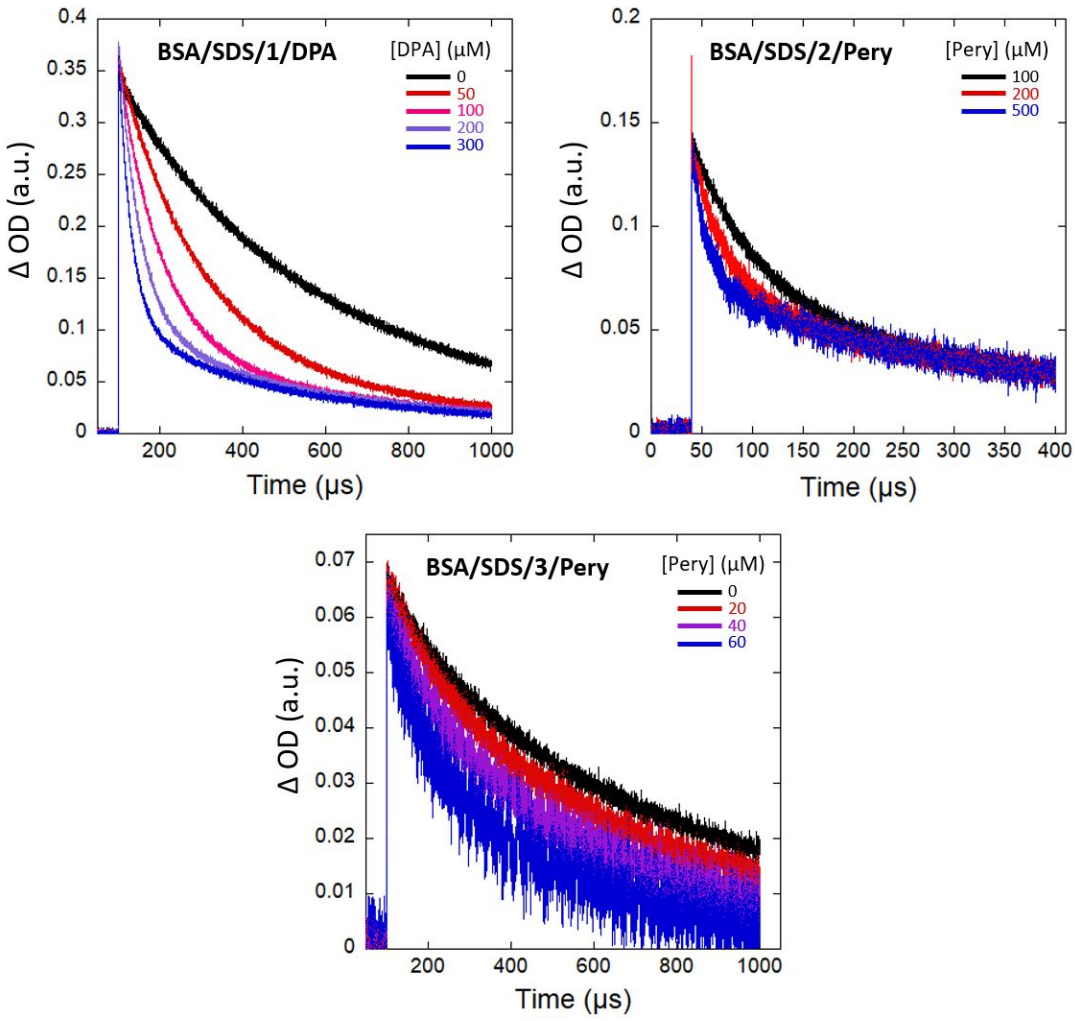

Figure S12. The triplet absorption decay profiles of BSA/SDS/upconverter hydrogels containing increasing annihilator concentrations. The triplet decay was measured at 430 nm for BSA/SDS/**1**/DPA and BSA/SDS/**3**/Pery hydrogels, and at 450 nm for BSA/SDS/**2**/Pery, following a 532 nm laser excitation pulse. The optimized reagent concentrations were used: [BSA] = 4.5 mM, [**1**] = 21.2 μM, [**2**] = 43.5 μM, and [**3**] = 14.7 μM. The above data were measured under aerobic conditions at room temperature.

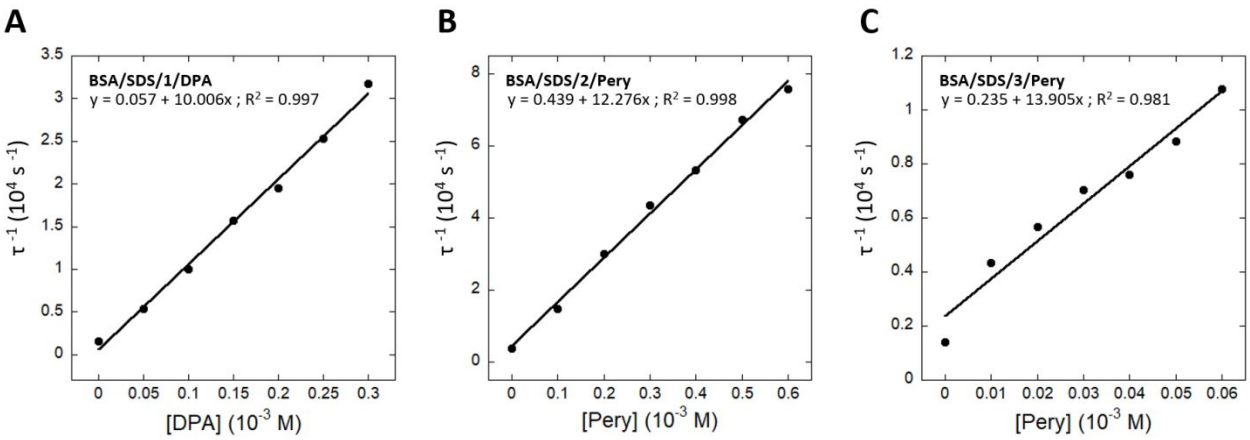

Figure S13. The Stern-Volmer plots for: (**A**) BSA/SDS/**1**/DPA, (**B**) BSA/SDS/**2**/Pery, and (**C**) BSA/SDS/**3**/Pery hydrogels. The optimized reagent concentrations were used: [BSA] = 4.5 mM, [**1**] = 21.2 μM, [**2**] = 43.5 μM, and [**3**] = 14.7 μM. The above data were measured under aerobic conditions at room temperature. The Stern-Volmer equation was used as the theoretical model for determining the quenching constant (k_q) of the sensitizer within the BSA/SDS hydrogel:

$$\frac{1}{\tau} = k_q[A] + \frac{1}{\tau_0}$$

Where τ is the sensitizer triplet excited state lifetime in the presence of varying annihilator (A) concentrations and τ_0 is thee sensitizer triplet excited state lifetime in the absence of annihilator. Using the k_q determined from the Stern-Volmer analysis, the TET efficiency (Φ_{TET}) for sensitizers **1-3** in the BSA/SDS hydrogel was calculated using the relationship below.

$$\Phi_{TET} = \frac{k_q[A]}{\frac{1}{\tau_0} + k_q[A]}$$

The Stern-Volmer and Φ_{TET} relationships were obtained from reference [4].

References

[1] Buck, J. T.; Boudreau, A. M.; DeCarmine, A.; Wilson, R. W.; Hampsey, J.; Mani, T. Spin-Allowed Transitions Control the Formation of Triplet Excited States in Orthogonal Donor-Acceptor Dyads. *Chem* **2019**, *5*, 138–155.

[2] Zhou, Q.; Zhou, M.; Wei, Y.; Zhou, X.; Liu, S.; Zhang, S.; Zhang, B. Solvent Effects on the Triplet–Triplet Annihilation Upconversion of Diiodo-Bodipy and Perylene. *Phys. Chem. Chem. Phys.* **2017**, *19*, 1516–1525.

[3] Singh, A.; Johnson, L. W. Phosphorescence Spectra and Triplet State Lifetimes of Palladium Octaethylporphyrin, Palladium Octaethylchlorin and Palladium 2,3-Dimethyloctaethylisobacteriochlorin at 77 K. *Spectrochim. Acta Part A Mol. Biomol. Spectrosc.* **2003**, *59*, 905–908.

[4] Turro, N. J.; Ramamurthy, V.; Scaiano, J. C. *Modern Molecular Photochemistry of Organic Molecules*; University Science Books, 2010.